Environmental (wet and dry) cycling of hydraulic lime mortars

Ryan Morgan and Richard Ball

Ryan C. Morgan is an undergraduate student in civil engineering at the Department of Architecture and Civil Engineering, University of Bath. He is an Institution of Civil Engineers Quest Scholar and currently works for John Sisk and Son Ltd as a trainee engineer. He is also a student member of the Institution of Structural Engineers.

Richard J. Ball BEng, PhD, CSci, CEng, MIMMM, FHEA, is a lecturer in the BRE Centre for Innovative Construction Materials, Department of Architecture and Civil Engineering, University of Bath. His research interests have focused on microstructure/macrostructure property relationships, setting reactions, degradation processes, and water transport mechanisms in lime-based binders. He is a committee member, and secretary, of the West of England Metals and Materials Association (WEMMA).

This study investigates the impact moisture control has on the aftercare of freshly manufactured hydraulic lime mortars by wet and dry cycling. Mechanical properties were monitored by periodic compressive testing and the extent of carbonation by phenolphthalein staining of cross sections. Hydration products after 28 days of cycling were identified by microstructural analysis using scanning electron microscopy. The cycling procedure caused a dramatic increase in compressive strength development. This was attributed to an increased rate of carbonation and hydration in three different mix designs containing aggregates with different particle size distributions. The cycling process also increased the depth of carbonation significantly. It was found that finer aggregates had greater depths of carbonation, in all exposure conditions. The strength development, as a result of 28 days of cycling, was similar in the fine- and mixed-particle aggregate mix designs since they were both fully carbonated, whereas the equivalent strength increase was lower for the coarse aggregate mix as the specimens weren't fully carbonated. This illustrates the importance of carbonation on strength development within hydraulic lime mortars, with a finer aggregate causing a faster strength increase.

Introduction

History of hydraulic lime mortars

Lime has been used as a binder in construction for thousands of years.[1] However, Portland cement, which emerged in the 19th century, promptly replaced lime mortar due to its ease of use, quick setting, and compressive strength.[2,3] Nonetheless, since cement mixes are often chemically different and too strong for the preservation of historic buildings, the need for a compatible material has promoted resurgence in the use of lime mortars.[4,5] This has led to an increase in awareness of the many environmental and structural benefits of lime mortars, and their suitability for both new build and conservation work.[6,7]

The development of hydraulic lime was advanced significantly at the start of the 20th century across the whole of Europe. Following the 19th-century work of Vicat et al., Platzmann undertook studies which outlined the classification, production, assets, and composition of hydraulic limes.[8–10] These studies illustrated that hydraulic lime mortars were of lower strength than Portland cement mortars, but of higher strength than air lime mortars.

Properties of hydraulic lime mortars

Building limes are available as high calcium (non-hydraulic) lime or hydraulic lime for construction.[11,12] High calcium lime is essentially calcium hydroxide, which hardens through the process of carbonation, whereas hydraulic lime contains calcium hydroxide and other compounds which react with water.[13,14] Natural hydraulic limes (NHL) contain reactive silicates formed from impurities such as clay during the burning process.

Hydraulic lime mortars achieve their strength through chemical set, hydration, and carbonation.[15,16] The hydration reaction is rapid in comparison with carbonation and is responsible for the initial set of hydraulic lime mortars.[17] Hydraulic limes are classified in BS EN 459-1: 2001 in ascending order of compressive strength as NHL 2, NHL 3.5, or NHL 5.[18] They have many advantages over Portland cement and air-lime-based mortars (both environmentally and structurally).[19,20] Lime mortar is commonly deemed to have a less detrimental impact on the environment than cement-based mortar amongst many other benefits, whilst hydraulic lime mortars have far greater structural performance than non-hydraulic lime mortars.[21–23]

Carbonation

Carbonation occurs in a hydraulic lime mortar when carbon dioxide dissolves in the pore water and forms carbonic acid, which subsequently reacts with calcium hydroxide to form calcium carbonate. This reaction is generally described by the equations below.

$$CO_2 + H_2O \rightarrow HCO_3^- + H^+$$

$$HCO_3^- \rightarrow CO_3^{2-} + H^+$$

$$Ca(OH)_2 \rightarrow Ca^{2+} + 2OH^-$$

$$Ca^{2+} + CO_3^{2-} \rightarrow CaCO_3$$

It is widely acknowledged that the rate of carbonation is influenced by a number of factors, including relative humidity (RH), temperature, and carbon dioxide concentration.[24]

Carbonation will not occur at very low RH, when the mortar is dry, since water is required for the reaction to occur.[25] However, a saturated mortar will slow down carbonation significantly, since carbonation is a diffusion-based process, and diffusion is roughly 10,000 times slower in water than it is in air.[26,27] Van Balen and Van Gemert suggested that 100% of the pore surface was available for carbonation between roughly 40 and 80% RH, with carbonation unable to take place in RH below 20% due to insufficient pore pressure for carbon dioxide diffusion. It was also specified that when RH is above 90%, less than 50% of the pore surface is available for carbonation.[28]

For carbonation to occur, carbon dioxide needs to dissolve in water, which implies that carbonation may act more efficiently at lower temperatures, since carbon dioxide is more soluble in water at lower temperatures.[29] However, chemical reactions in general are faster at higher temperatures. Van Balen et al. suggested that the optimum carbonation speed is found at around 20°C.[30]

Allen and Ball reported that compressive strength of lime mortar cured in nitrogen, containing 400ppm carbon dioxide, was significantly higher than when it was cured in pure nitrogen at different ages, due to increased carbonation.[31] Furthermore, El-Turki et al. demonstrated that the rate of carbonation within hydraulic lime mortars increased as the carbon dioxide concentration was raised from 400ppm to 4%, which suggested that the higher the concentration of carbon dioxide, the faster the rate of carbonation.[32] Moreover, as is the case with many diffusion processes, the depth of carbonation is directly proportional to the square root of time.[33]

El-Turki et al. showed that, for both hydraulic lime and air lime mortars, the rate of carbonation decreases as the sand particle size is increased. It was shown that if the total surface area of the sand is reduced by increasing the particle size, fewer sites for the nucleation of calcite are available.[34]

Hydration

Hydration is a reaction of compounds with water to produce a hydrate, and is considered a chemical as well as a physio-mechanical change to the mortar.[35–37] Primarily, the hydration reaction consists of di-calcium silicate ($2CaOSiO_2$ [C_2S]) reacting with water to form calcium silicate hydrate ($3CaO.2SiO_2.3H_2O$ [C-S-H]), as is shown in the following equation:

$$2(2CaOSiO_2) + 4H_2O \rightarrow 3CaO.2SiO_2.3H_2O + Ca(OH)_2$$

In contrast to carbonation, hydration is primarily related to temperature and humidity.[38] By definition, the presence of water is essential for hydration to occur, thus hydration will not occur in completely dry conditions. Hydraulic lime mortars can set when they are under water, with the hydration reaction still occurring even when the material is saturated. Furthermore, since it is widely acknowledged that chemical reactions in general occur at a faster rate as temperature is increased and hydration doesn't rely on the solubility of carbon dioxide for the reaction to occur, it suggests the optimum temperature for hydration would be higher than for carbonation.

Environmental cycling

The exposure of a hydraulic lime mortar to wetting and drying is understood to have a positive impact on carbonation and hydration rates and consequently strength development.[39] If the mortar dries out rapidly it will lose its binding properties, increasing the chance of premature failure. Recently, a method of damping down termed 'tending' has become an increasingly popular method for wetting down mortar, which involves using a portable pressure pump to spray the surface of a mortar to prevent rapid drying. Tending creates a simulated wetting and drying cycle. It is impracticable to monitor on site the effect this cycling process has upon the compressive strength of lime mortar and how many cycles it is necessary to perform, although it is essential to optimise the initial exposure conditions in order to exploit lime's natural properties.

When a hydraulic lime mortar is dry, carbon dioxide will diffuse at a fast rate into the specimen. However, insufficient water is available for the formation of the carbonic acid required to promote carbonation (Figure 1a). As the mortar is wetted, the sample will become saturated, and the diffusion rate of carbon dioxide will reduce (Figure 1b).[40,41] Throughout the drying process the pore water gradually evaporates. At a critical point during the drying stage, pores will contain a thin film of water; this promotes carbonation but also enables diffusion of carbon dioxide (Figure 1c).[42] At this point the carbonation rate will be optimised.

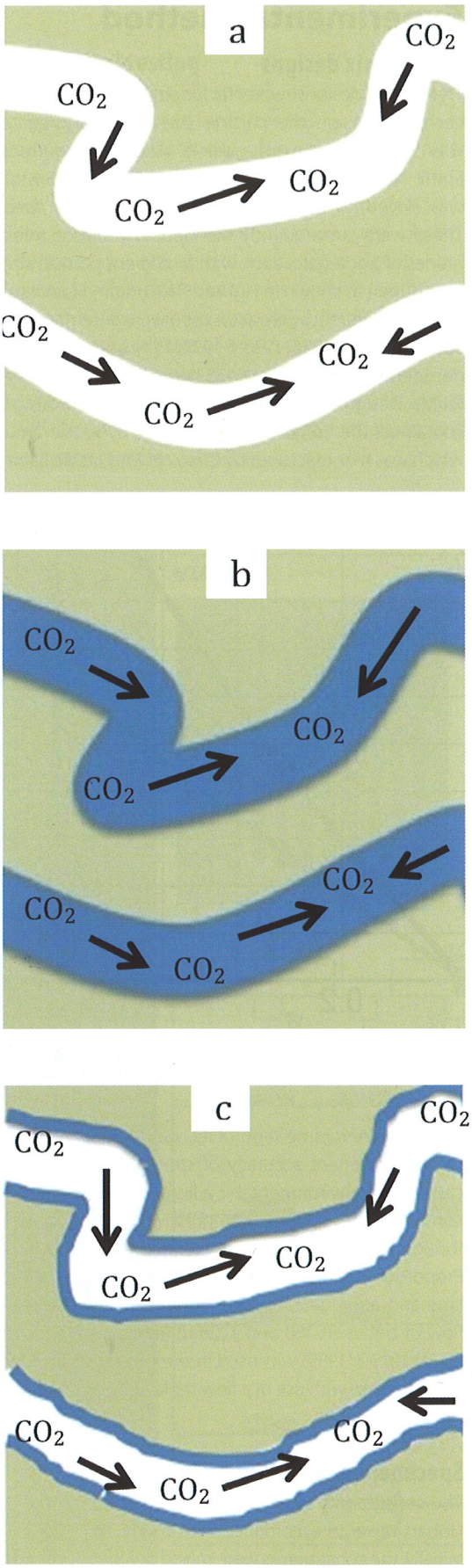

Fig. 1 Schematic diagram representing water presence in lime mortars during the cycling process: **a** completely dry pores; **b** saturated pores; **c** pores coated in a thin layer of water (optimum condition for carbonation).

Experimental method

Sample mix designs

Three mix designs were included in this study. In each mix design the particle size of the aggregate was varied. Sand with particle sizes ranging from 5mm to dust, supplied by Stone Supplies, Bristol, was sieved to separate the different particle sizes. These were subsequently blended to produce three grades of aggregate, each with a different particle size distribution as shown in Figure 2. The grading curves of the three different aggregates used were determined in accordance with BS EN 933-1: 1997.[43] The aggregate bulk densities were 1373kg/m^3, 1353kg/m^3, and 1490kg/m^3 for Mix Designs 1, 2, and 3 respectively. Each mix design contained the same binder, NHL 3.5 hydraulic lime, which was manufactured by Chaux et Enduits de Saint-Astier. A B/A volume ratio of 1:1 was used to increase the measurement accuracy of strength development caused by environmental cycling, as higher binder content creates a higher compressive strength,[44] even though site practice typically employs leaner ratios. Proportions were determined from dry volumes of the lime and aggregate. A water content that provided a flow of between 160 and 170mm (in accordance with BS EN 1015-3: 1999) was used in the mortar mixes. This was achieved with use of a flow table (in line with BS EN 1015-3: 1999).[45, 46]

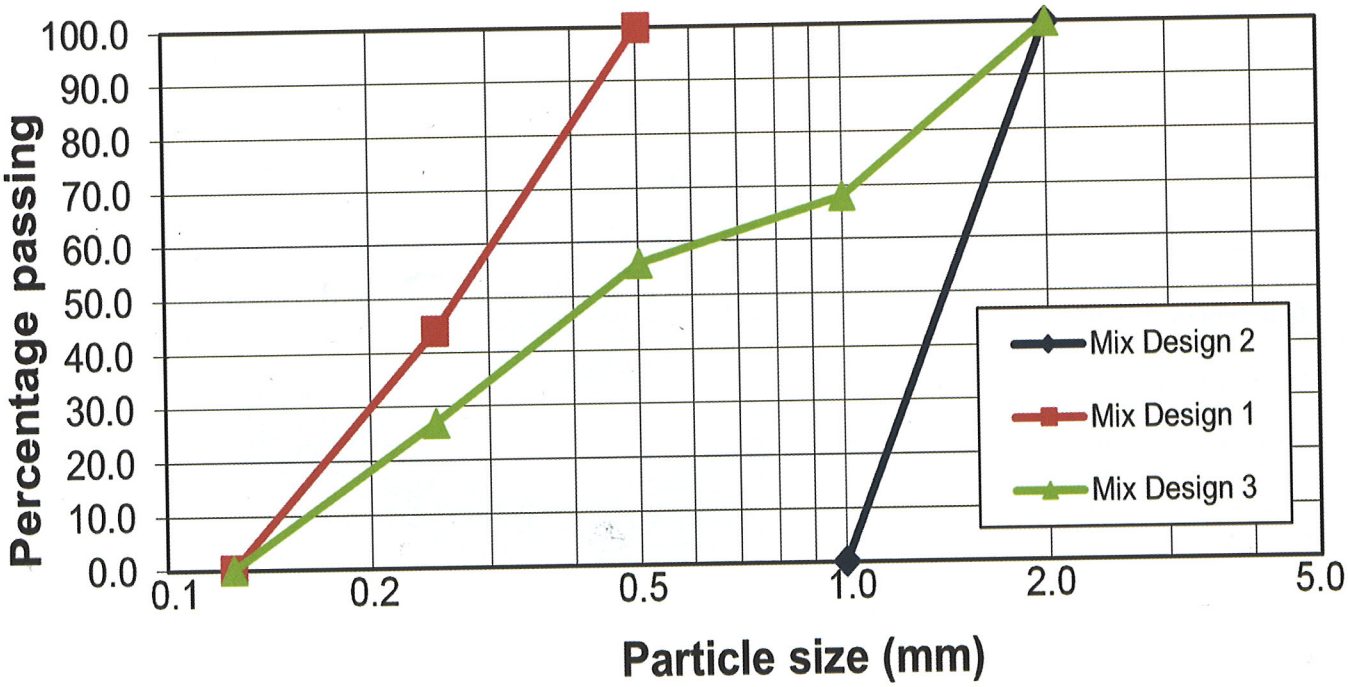

Fig. 2 Particle size distribution for aggregates used in Mix Designs 1, 2, and 3.

Specimen preparation

The constituents of each mix design were mixed in a Hobart mixer in accordance with BS EN 196-1: 2005.[47] Initially, the constituents were mixed dry for 60 seconds, and thereafter water was carefully added and mixing was continued for a period of 10 minutes. Cylindrical plastic moulds, 18mm in diameter by 36mm in length, were used to cast the mortar specimens. This specimen size is smaller than the widely used 40 x 40 x 160mm prisms and benefited from a shorter path for gaseous and moisture diffusion. This allowed the environmental cycling process to be studied within a practical time frame. The moulds were coated with release oil before the mortar was cast. To avoid the build-up of air pockets within the specimens, each specimen was cast in three layers, with each layer being tamped 20 times by means of a 5mm diameter Perspex tamper. The specimens were left to harden under laboratory conditions of 20±2°C and 65±5% RH. To ease extraction of the specimens, the moulds had a removable bottom and could be split along the sample length. The bottom of the mould was removed after one day of curing, and after seven days the mould was detached to remove the cylindrical specimens. All of the specimens were capped top and bottom using a thin layer of gypsum-based dental plaster, to provide parallel and flat surfaces. This action helped to distribute the compressive forces evenly during loading, and minimise localised stress concentrations.

Exposure conditions

After de-moulding, half of the specimens remained under laboratory conditions (20±2°C and 65±5% RH), while the other half were positioned in a purposely designed wetting and drying chamber. The selection

of specimens for each batch was randomised in order to reduce systematic errors. The chamber consisted of a spraying device capable of saturating the specimens within 60 seconds. Two fans, positioned to suck air through the chamber, dried the specimens over a period of several hours. Both spraying and drying operations were electronically controlled for a predefined duration of 10 minutes for wetting and 20 hours for drying, repeatedly for the duration of exposure within the chamber. The wetting and drying chamber arrangement is shown in Figure 3. Mix Designs 1 to 3, both laboratory-controlled and environmentally cycled, were analysed on Days 0, 1, 3, 7, 14, and 28, with Day 0 being the day in which the specimens were de-moulded.

Mechanical testing

For all mix designs, six specimens of each exposure condition (controlled and cycled) were tested in compression on each day of investigation, in order to reduce potential systematic errors in this study. Each specimen was loaded until failure using a 50kN Tritech testing machine with stainless steel platens. The top platen was able to move about a central ball joint to accommodate specimens in which the top and bottom surfaces were not parallel. A load compressed the specimens at a rate of 1mm/min, and displacement was measured to an accuracy of 0.001mm, whilst the load cell recorded loads to an accuracy of 0.1N. Values of load and displacement were automatically logged during the compressive tests.

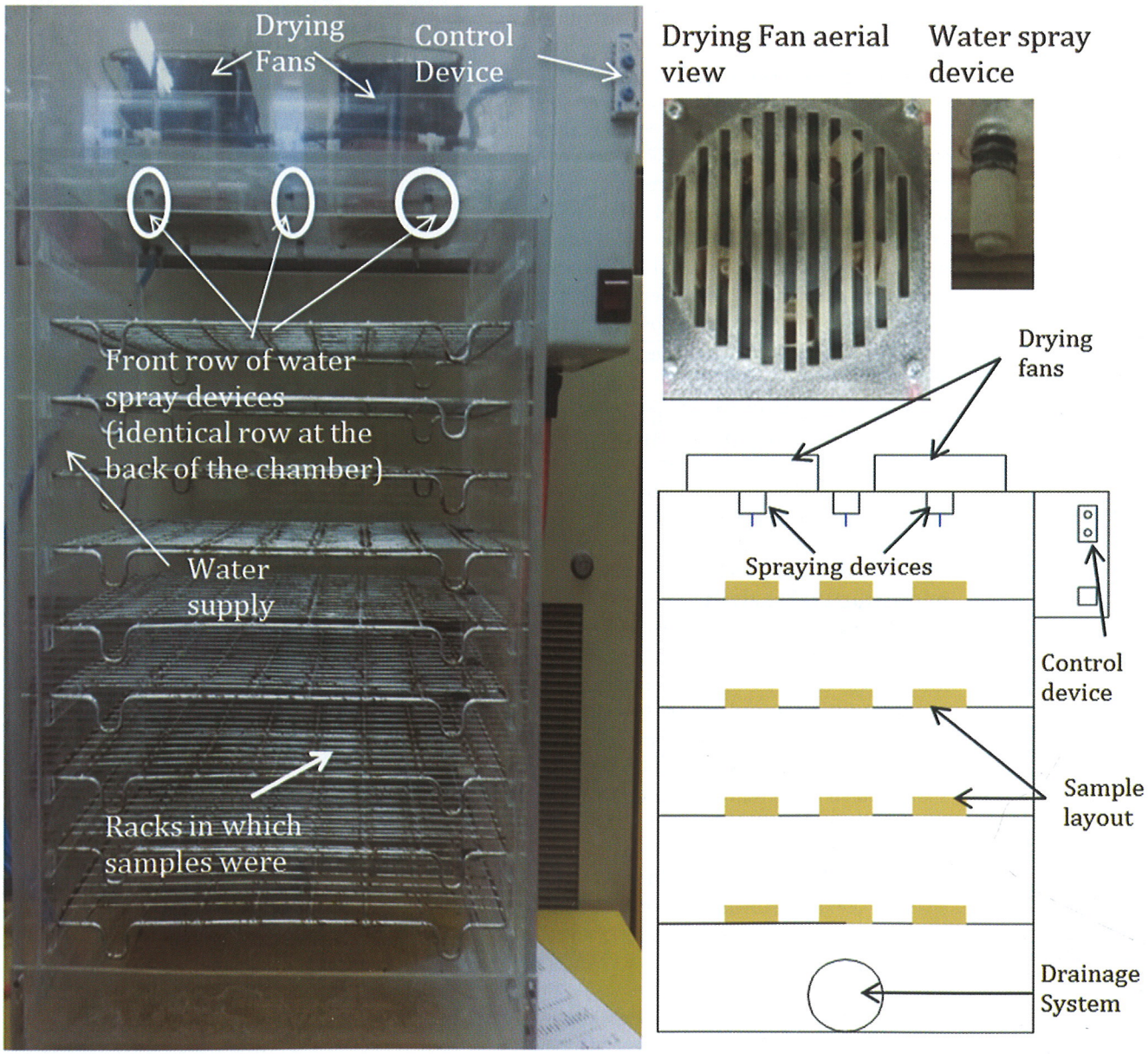

Fig. 3 Wetting and drying chamber.

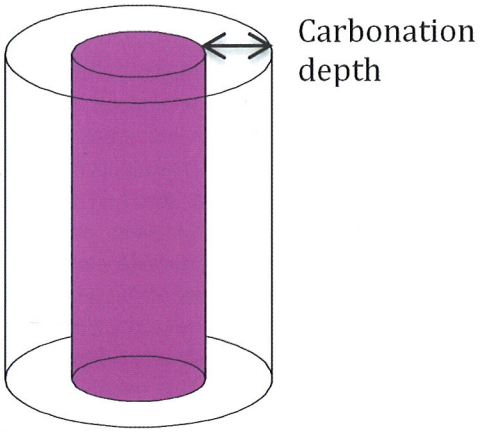

Fig. 4 Schematic diagram illustrating carbonation depth revealed by phenolphthalein staining assuming no carbon dioxide diffusion through capping material (not shown).

Phenolphthalein staining

The general mode of failure resulted in the mortar specimens breaking into two evenly sized sections. Straight after the compressive strength tests, carbonation of all of the mortar specimens was evaluated by spraying a 1% solution phenolphthalein in ethanol onto a fresh fracture surface. A schematic diagram illustrating carbonation depth is shown in Figure 4. The pink stained area indicates the presence of high-alkalinity uncarbonated calcium hydroxide, whereas the clear, uncoloured area represents lower-alkalinity calcium carbonate. There was a clear boundary between the carbonated and uncarbonated regions in all specimens. The diameter of each sample was measured prior to the compressive tests, then after each compressive test the diameter of the stained area on the fracture surface was measured. These measurements were completed using a digital caliper, which could record values to an accuracy of 0.01mm. A photo of each stained specimen was also taken, to form a visual log of the depth of carbonation within the different mortar specimens.

Optical microscopy and microstructural analysis

Optical microscope imaging of polished cross sections was performed using a Leica M205C microsystem with zoom range of 7.8 to 160x. Microstructural analysis was undertaken using a JEOL JSM-6480LV scanning electron microscope. Polished cross sections were analysed using backscattered electron imaging under a low vacuum mode with a 15kV accelerating voltage. Fracture surfaces were examined using secondary electron images. They were coated in a layer of gold for two minutes in an Edwards sputter coater and were analysed using a secondary electron detector, in a high vacuum mode, at an accelerating voltage of 10kV. Estimates of the sample porosities were determined from representative cross sectional images. ImageJ image analysis software was used to identify and quantify pores based on their cross-sectional area.

Results and discussion

Mix design classification

Optical microscope images showing the differences between the mix designs are given in Figure 5. The images reveal how the aggregate size varied between the mix designs, with a noticeable increase in aggregate/binder interfacial surface area and thus more nucleation sites in Mix Design 1. The aggregate in Mix Design 3 was evidently well graded and had a larger variance in aggregate size than in Mix Designs 1 and 2. The proportion of the surface that is aggregate was much greater in Mix Design 1, whilst the spacing between aggregate particles was largest in Mix Design 2.

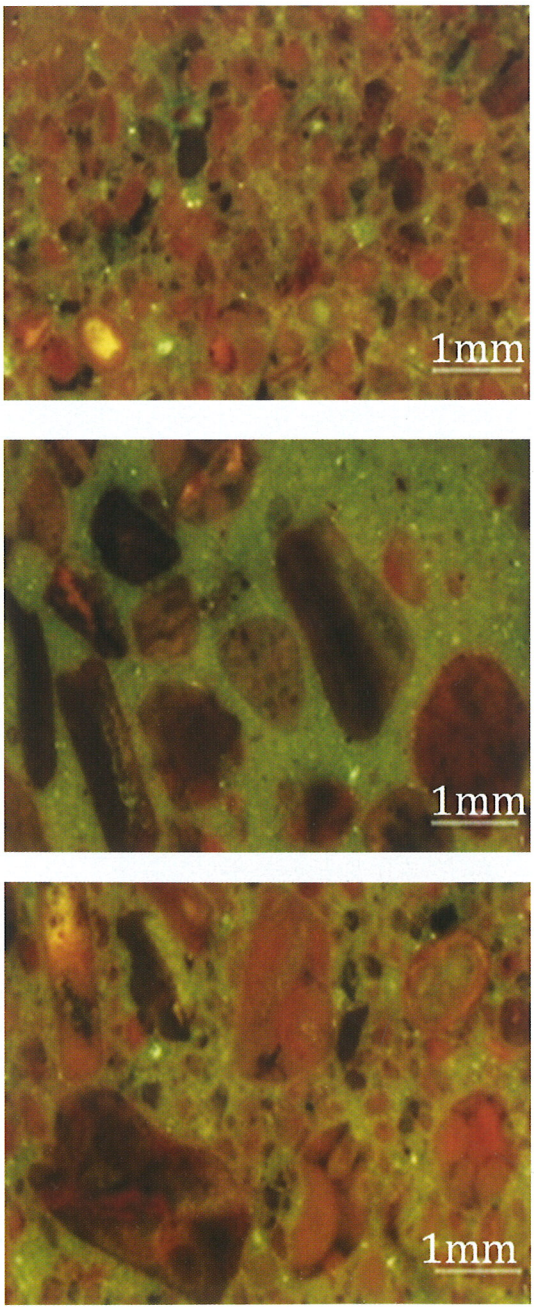

Fig. 5 Optical microscope images: **a** Mix Design 1; **b** Mix Design 2; **c** Mix Design 3.

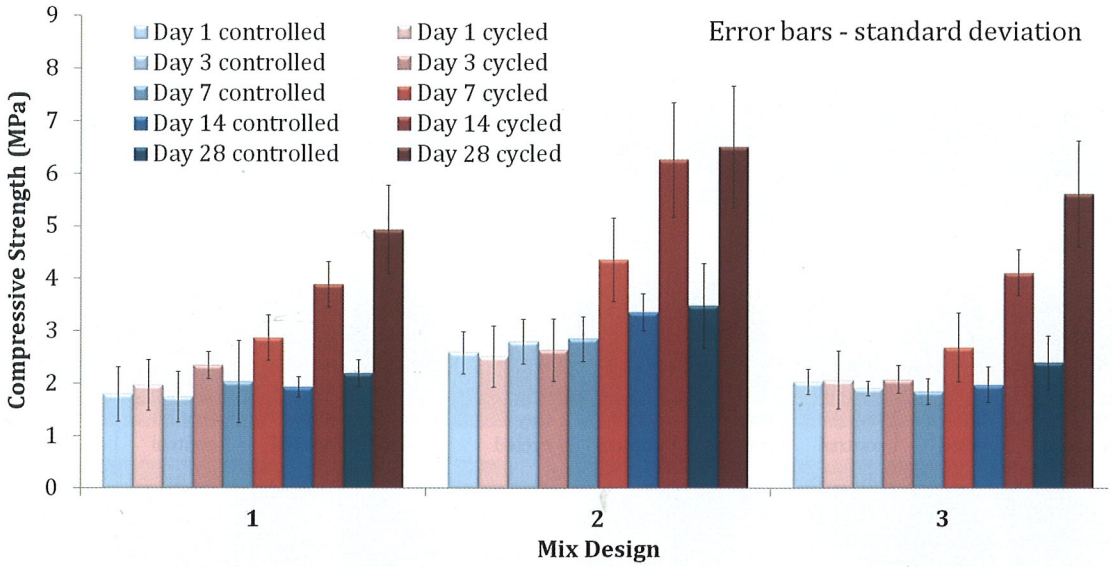

Fig. 6 Compressive strength enhancement due to wet and dry cycling of mortar in Mix Designs 1, 2, and 3.

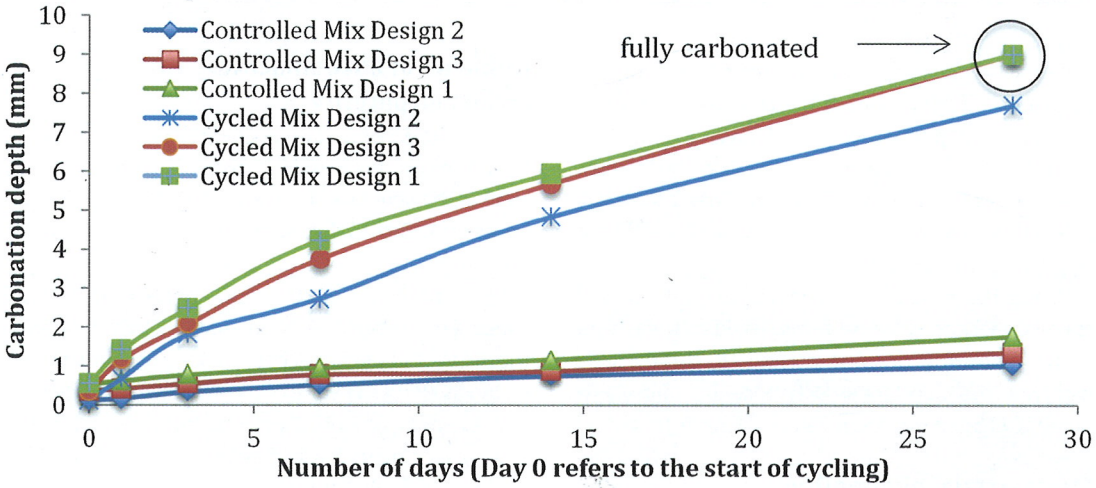

Fig. 7 Average depth of carbonation for each mix design on each investigation day.

Compressive strength of specimens

The compressive strengths of control and cycled specimens are set out in Figure 6, which shows a significant strength increase as a result of cycling for all mix designs. Mix Design 2 had the highest initial strength and the highest strength after the cycling process; however, the percentage increase of strength due to cycling was higher in Mix Designs 1 and 3. The compressive strength of the control specimens remained almost constant throughout the 28 days.

Variations in the rate of strength increase over the 28-day cycling period are determined by differences in the mix design as well as the rate of absorption and evaporation of the different mortar specimens. The major strength increase as a result of cycling was observed between 7 and 14 days for Mix Designs 2 and 3. This is in agreement with El-Turki et al., who suggested the strength development in hydraulic lime mortars, caused by cycling, is delayed as a result of preferential hydration.[48] In addition, the formation of silicates, as a result of hydration, will hinder water transportation within the mortar, reducing strength development from carbonation. However, in Mix Design 1 a fairly significant increase in strength was observed after 3 days of environmental cycling. This correlates with the increased depth of carbonation for Mix Design 1, after 3 days of cycling, in comparison with Mix Designs 2 and 3 (Figures 6 and 7). The finer aggregate contained in Mix Design 1 created an increased number of sites for reaction within the mortar, so there was greater opportunity for carbonation to occur simultaneously with hydration.

Carbonation depth

Figure 7 shows the increase in carbonation depth as a result of wetting and drying. The carbonation front progressed at the highest rate in Mix Design 1 for both the control and cycled specimens. Mix Design 2 showed the slowest carbonation. This is in agreement with the work of El-Turki et al., who observed an increase in

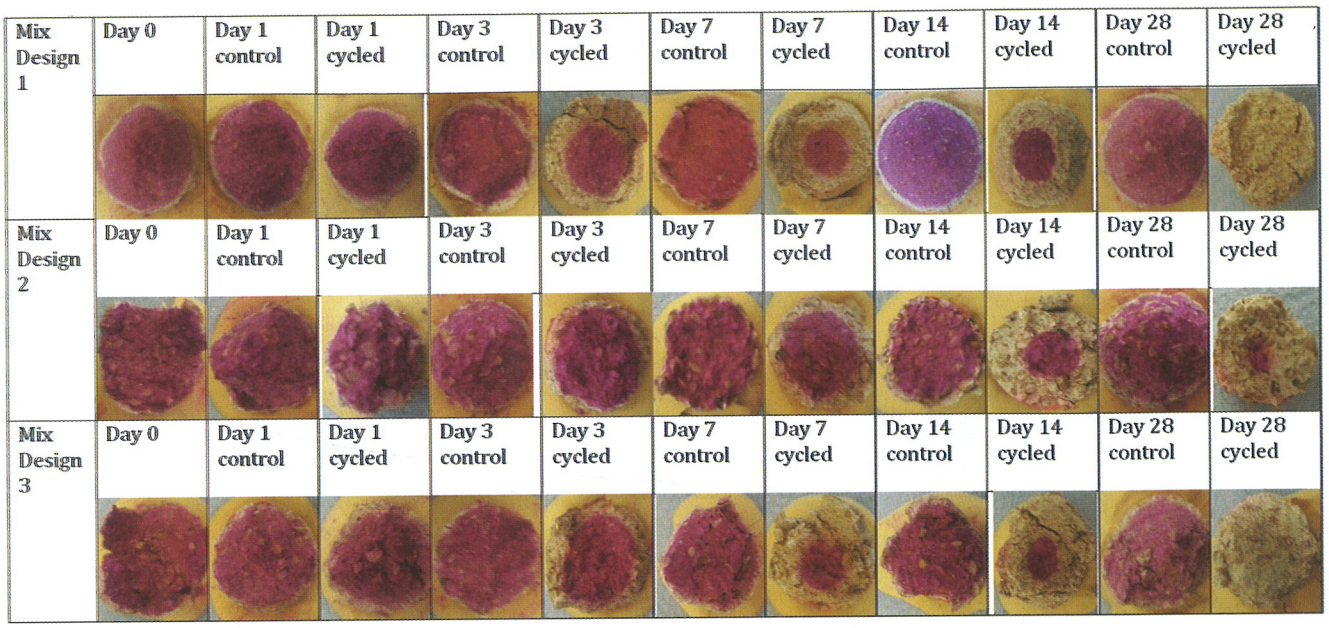

Fig. 8 Representative phenolphthalein-stained cross sections of laboratory controlled and environmentally cycled specimens of Mix Designs 1, 2, and 3.

carbonation rate in specimens with smaller aggregate particle size.[49] Specimens of Mix Designs 1 and 3 were fully carbonated after 28 days of cycling, suggesting this may be an optimal cycling period. In comparison, specimens of Mix Design 2 weren't fully carbonated after 28 days of cycling, which was attributed to its larger aggregate particle size.

A visual timeline of representative phenolphthalein-stained specimens for each mix design on each day of investigation is detailed in Figure 8. These images highlight the substantial difference in carbonation depths between the control and cycled specimens.

Stress–strain relationship

Representative stress–strain curves for Mix Designs 1 and 2 (both cycled and controlled) on Day 14 of the investigation are shown in Figure 9. Cycling led to a marginal increase in specimen stiffness, which may be attributed to changes in pore size as a result of cycling.

Influence of environmental cycling on porosity

A reduced porosity was evident in all mix designs following environmental cycling. Figures 10 to 12 show representative backscattered electron images for control and cycled specimens respectively at 28 days. A greater number of pores were evident in the control specimens. Furthermore, pores in the cycled specimens showed less interconnectivity, whereas those in the control specimens formed extended pore channels along the edge of the aggregate particles.

A greater number of pores were observed in Mix Design 1 compared with Mix Designs 2 and 3, which could be the reason for the lower initial strength of Mix Design 1 specimens. The average porosity of each mix design on Day 28 of analysis is given in Figure 13. Carbonation and hydration alter the microstructure of air lime mortars, thus influencing their water transportation properties.[50,51] This study confirms that

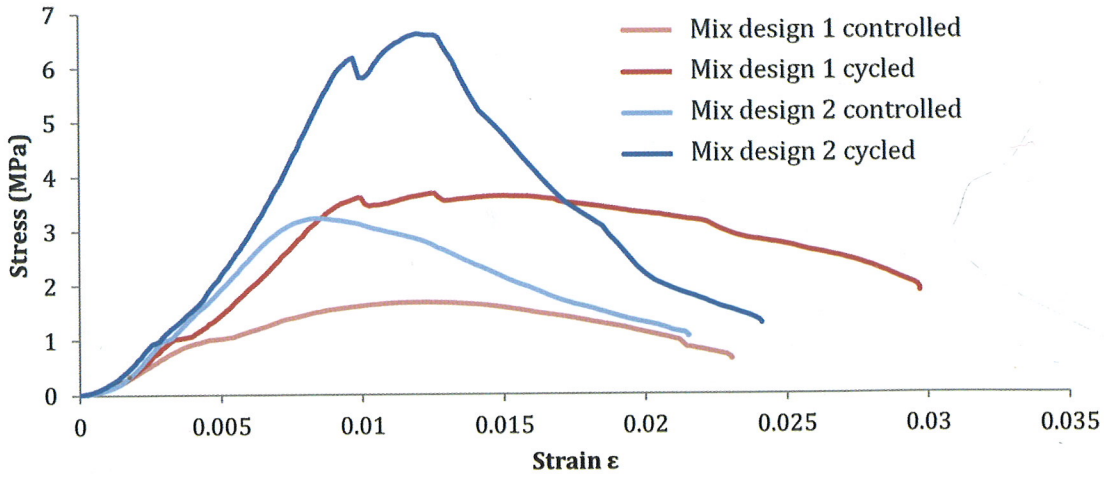

Fig. 9 Typical stress–strain curves at 14 days for laboratory controlled and environmentally cycled specimens of Mix Designs 1 and 2.

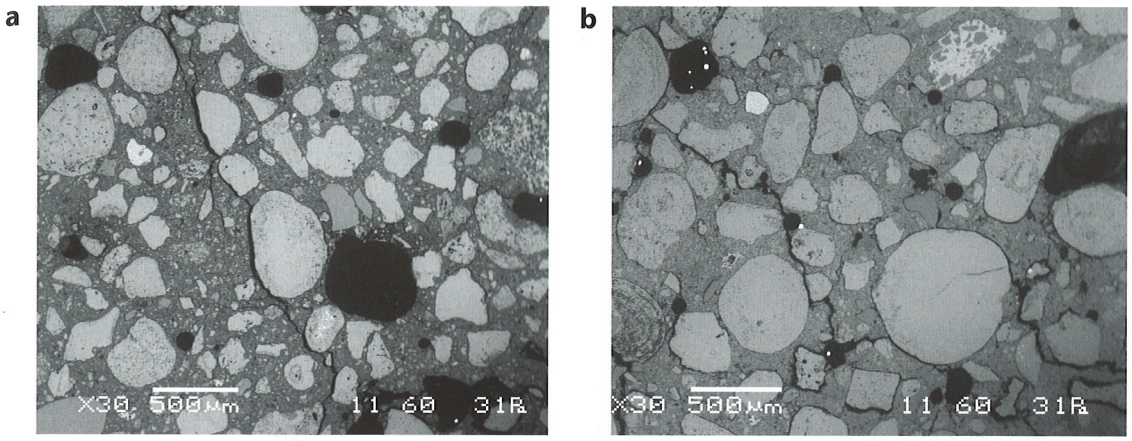

Fig. 10 Backscattered electron images of the internal surface of Mix Design 1 after: **a** 28 days laboratory controlled; **b** 28 days environmentally cycled.

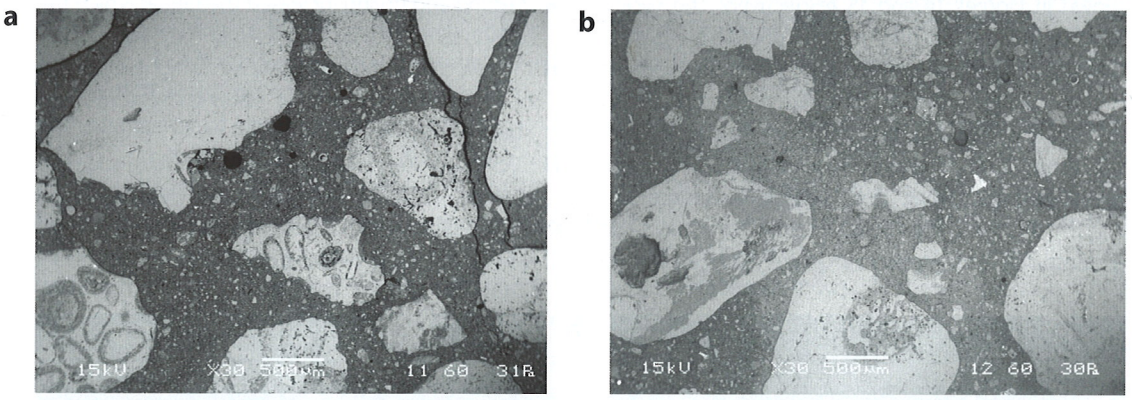

Fig. 11 Backscattered electron images of the internal surface of Mix Design 2 after: **a** 28 days laboratory controlled; **b** 28 days environmentally cycled.

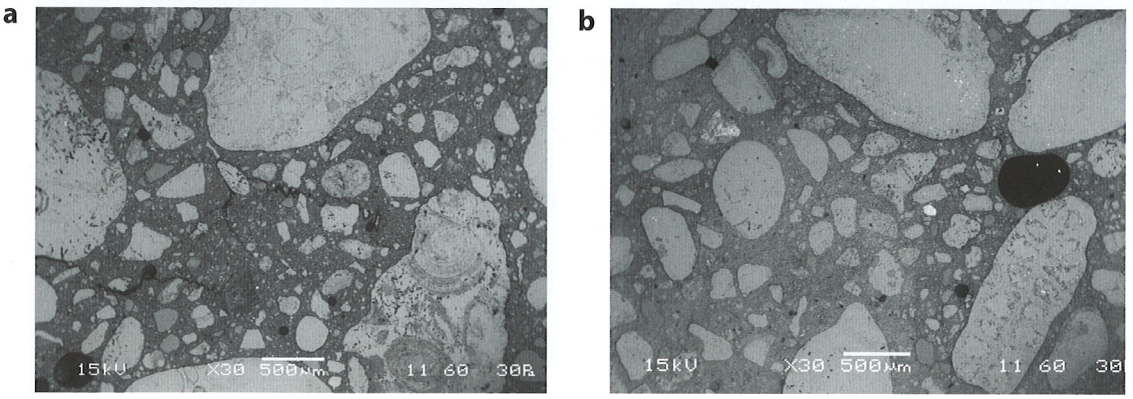

Fig. 12 Backscattered electron images of the internal surface of Mix Design 3 after: **a** 28 days laboratory controlled; **b** 28 days environmentally cycled.

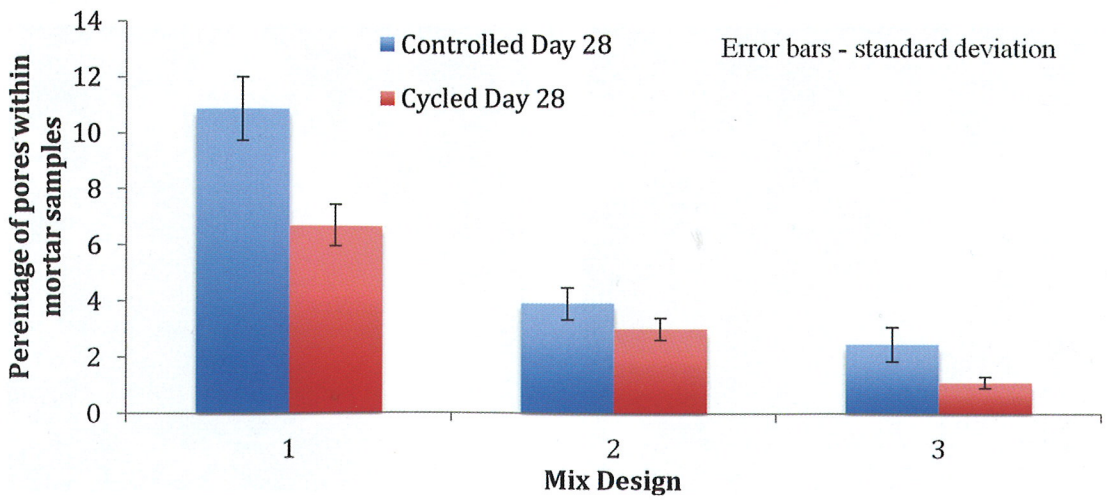

Fig. 13 Percentage porosity of Mix Designs 1, 2, and 3 at 28 days.

the relationship also applies to hydraulic lime mortars, with the enhanced rate of carbonation and hydration in the environmentally cycled specimens, leading to reduced porosity. The enhanced rate of carbonation and hydration also improved the bond strength between the aggregate and binder, with the backscattered electron images showing a greater number of pore channels at the binder/aggregate interface within the control specimens (Figures 10 to 12).

Microstructural analysis

Secondary electron SEM images of typical microstructures of control and cycled specimens of Mix Designs 1 and 2 at Day 28 of the investigation are shown in Figures 14 and 15 respectively. The cycled structures were less porous and contained a greater number of tightly packed crystals, which are believed to be carbonate. Calcium carbonate crystals nucleated and grew in the surface of aggregate particles, and silicate phases developed across voids in cycled specimens, decreasing pore volume and pore size and creating a more interconnected structure. The greatest difference in microstructure between control and cycled specimens was found in specimens of Mix Design 1. This was attributed to the finer aggregate creating more sites for nucleation.

Conclusions

The following conclusions can be drawn from the results presented:

- Wetting and drying increased the compressive strength of newly manufactured hydraulic lime mortars. The increased strength of cycled specimens was attributed to hydration and carbonation processes.
- Wetting and drying increased the rate at which the carbonation front progressed into the sample.
- Mortars containing aggregate with a high proportion of fine particles exhibited faster carbonation and strength development.
- Cycled specimens had a reduced pore size and pore volume.
- Cycled specimens had an increased stiffness, which was attributed to reduced porosity.

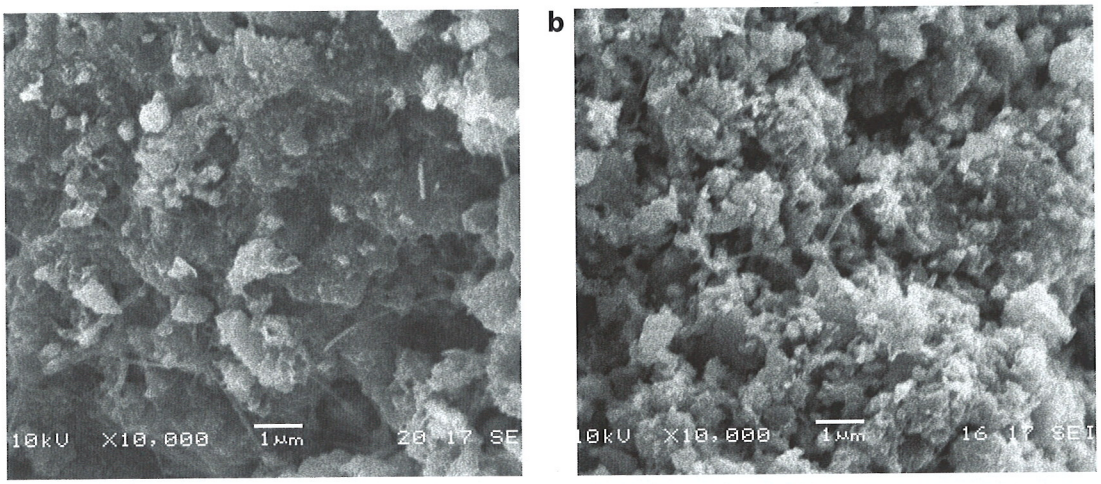

Fig. 14 Secondary electron images of the internal structure of Mix Design 1 after: **a** 28 days laboratory controlled; **b** 28 days environmentally cycled.

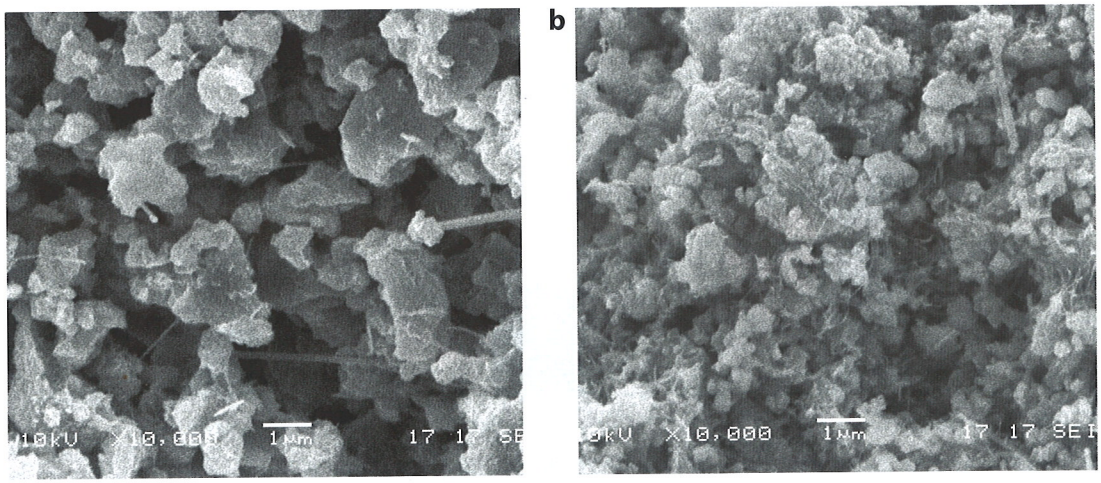

Fig. 15 Secondary electron images of the internal structure of Mix Design 2 after: **a** 28 days laboratory controlled; **b** 28 days environmentally cycled.

References

1 Boynton, R. S., *Chemistry and technology of lime and limestone*, 2nd edn, New York, John Wiley and Sons, 1980.
2 Bye, G. C., *Portland cement: composition, production and properties*, 2nd edn, London, Thomas Telford Publishing, 1999.
3 Hewlett, P. C., *Lea's chemistry of cement and concrete*, London, Edward Arnold, 1998.
4 Davey, N., *A history of building materials*, New York, Drake Publishers, 1971.
5 Allen, G. C., Allen, J., Elton, N., Farey, M., Holmes, S., Livesey, P., and Radonjic, M., *Hydraulic lime mortar for stone, brick and block masonry: a best practice guide*, Shaftesbury, Donhead Publishing, 2003.
6 Holmes, S. and Wingate, M., *Building with lime – a practical introduction*, London, Intermediate Technology, 1997.
7 Hughes, P., *The need for old buildings to breathe*, London, Society for the Protection of Ancient Buildings, 1986.
8 Vicat, L. J., Hawkesworth, J., and Smith, J. T., *Mortars and cements*, Routledge, 1997 (facsimile of 1837 edn).
9 Platzmann, C. R., 'Continental natural and artificial hydraulic limes' in *Cement and Lime Manufacture* Vol. 11, No. 4, 1938, pp. 67–72.
10 Platzmann, C. R., 'Hydraulic limes, natural and artificial' in *Rock Products* Vol. 27, No. 23, 1924, pp. 49–51.
11 See 5 above.
12 BS EN 459-1: 2010 *Building lime. Definitions, specifications and conformity criteria*, British Standards Institution.
13 Lanas, J., Pérez Bernal, J. L., Bello, M. A., and Alverez Galindo, J. I., 'Mechanical properties of natural hydraulic lime-based mortars' in *Cement and Concrete Research* Vol. 34(12), 2004, pp. 2191–2201.
14 Lea, F. M., *The chemistry of cement and concrete*, Edward Arnold, 1970.
15 Ashurst, J., 'The technology and use of hydraulic lime' in *The Building Conservation Directory*, Cathedral Communications, 1997.
16 Schofield, J., *Lime in building: a practical guide*, Black Dog Press, 1997.
17 Cowper, A. D., *Lime and lime mortars*, BRE Special Report No. 9, 1927, reprinted by Donhead Publishing, 1998.
18 See 12 above.
19 See 17 above.
20 Zhou, Z., 'Development of bond strength in hydraulic lime mortared brickwork', PhD thesis, University of Bath, 2012.
21 See 16 above.
22 See 17 above.
23 See 20 above.
24 El-Turki, A., Ball, R. J., and Allen, G. C., 'The influence of relative humidity on structural and chemical changes during carbonation of hydraulic lime' in *Cement and Concrete Research* Vol. 37, 2007, pp. 1233–40.
25 Arandigoyen, M., Lanas, J., and Alvarez, J. J., 'Carbonation of lime-cement mortars: a description of this process through the fractal dimension' in *Proceedings of the 10th international congress on deterioration and conservation of stone*, eds Kwiatkowski and Lifvendahl, Stockholm, ICOMOS, pp. 1057–64.
26 Houst, F. Y., 'The role of moisture in the carbonation of cementitious materials' in *International Journal for Restoration of Buildings and Monuments* Vol. 2, 1996, pp. 49–66.
27 El-Turki, A., Carter, M. A., Wilson M. A., Ball, R. J., and Allen G. C., 'A microbalance study of the effects of hydraulicity and sand grain size in carbonation of lime and cement' in *Construction and Building Materials* Vol. 23(3), 2009, pp. 1423–8.
28 Van Balen, K. and Van Gemert, D., 'Modelling lime mortar carbonation' in *Materials and Structures* Vol. 27(7), 1994, pp. 393–8.
29 Dodds, W. S., Stutzman, L. F., and Sollami, B. J., 'Carbon dioxide solubility in water' in *Journal of Chemical and Engineering Data* Vol. 1, 1956, pp. 92–5.
30 Van Balen, K., 'Carbonation reaction of lime kinetics at ambient temperature' in *Cement and Concrete Research* Vol. 35(4), 2005, pp. 647–57.
31 Allen, G. C. and Ball, R. J., 'Mechanical properties of hydraulic lime mortars' in APFAC, 4th Portuguese Congress on Mortars and ETICS, Auditório LNEC, Lisbon, 2012.
32 El-Turki, A., Ball, R. J., and Allen, G. C., 'Chemical and mechanical properties of lime-based mortar materials' in *The Journal of the Building Limes Forum* Vol. 13, 2006, pp. 71–87.
33 See 28 above.
34 See 27 above.
35 See 3 above.
36 Lawrence, M., 'A study of carbonation in non-hydraulic lime mortars', PhD thesis, University of Bath, 2006.
37 El-Turki, A., Ball, R. J., Holmes, S., Allen W. J., and Allen, G. C., 'Environmental cycling and laboratory testing to evaluate the significance of moisture control for lime mortars' in *Construction and Building Materials* Vol. 24, 2010, pp. 1392–7.
38 See 37 above.
39 See 37 above.
40 See 26 above.
41 See 27 above.
42 See 37 above.
43 BS EN 933-1: 1997 *Tests for geometrical properties of aggregates. Determination of particle size distribution. Sieving method*, British Standards Institution.
44 See 13 above.
45 See 37 above.
46 BS EN 1015-3: 1999 *Methods of test for mortar for masonry. Determination of consistence of fresh mortar (by flow table)*, British Standards Institution.
47 BS EN 196-1: 2005 *Methods of testing cement. Determination of strength*, British Standards Institution.
48 See 37 above.
49 See 27 above.
50 Lawrence, M., Mays, T., Rigby, S., Walker, P., and D'Ayala, D., 'Effects of carbonation on the pore structure of non-hydraulic lime mortars' in *Cement and Concrete Research* Vol. 37(7), 2007, pp. 1059–69.
51 El-Turki, A., Ball, R. J., Carter, M. A., Wilson, M. A., Ince, C., and Allen, G.C., 'Effect of dewatering on the strength of lime and cement mortars' in *Journal of the American Ceramic Society* Vol. 93, 2010, pp. 2074–81.